Application of Design Simulation and Experimental Design Methodologies to the Study of Coronary Stent Designs

Jared May[1], Nilesh N. Joshi*[2] and Rajeev Nair[3]
Dept. of Applied Engineering & Technology
Morehead State University

[1]Morehead State University, jdmay@moreheadstate.edu
[2]Morehead State University, n.joshi@moreheadstate.edu
[3]Morehead State University, r.madhavann@moreheadstate.edu

ABSTRACT

Design Simulation and Experimental Design are widely used techniques in engineering design studies. Design simulation is useful in the virtual testing of new designs without having to spend resources on creating actual prototypes. Experimental Design is useful in analyzing relationships between various parameters of a design and their impact on the functionality and reliability of the design. In this paper, we use a combination of these two techniques to analyze coronary stent designs. A stent is a medical device used to improve blood flow in certain diseased human arteries. Many different stent designs exist in the market. These designs vary in the core structure of the stent and the material used. Optimal selection of the design features plays an important role in the robustness and longevity of stents exposed to various pressures within the artery. This is especially true for the coronary stent design. A coronary stent constitutes critical parameters such as strut design variables, strut size factors like its thickness, and material that must be optimized. Using design simulation and experimental design, we study the effect and interactions of strut design and material on a deployed stent.

Keywords: stent, strut design, artery, design simulation, experimental design.
DOI: 10.3722/cadaps.2012.439-455

1 INTRODUCTION AND BACKGROUND

Heart related illnesses are the leading cause of death in the United States. In fact, some 81 million people are affected by heart disease in the United States [3]. Heart attacks and strokes are ailments

caused by severe arterial blockages. Stenting provides a means to alleviate these blockages and reduce the risk of heart attack and stroke.

Plaque buildup in the artery leads to a condition known as atherosclerosis. Atherosclerosis can harden the artery and eventually block the passage of blood through the artery. Stents are devices that are designed to reopen the lumen and allow for continued blood flow by expanding inside the artery. An expanded stent applies pressure to the fatty plaque that forms along the arterial walls. This pressure compresses the plaque and reopens the artery. Stents are designed to have high radial strength that allows them to act as scaffolding. This scaffolding nature and the fact that the lumen is reopened allows for continued blood flow.

The stent market has a total value of $7 billion. A total of one million stents are implanted each year. Therefore, there is a great potential for innovation in the stent industry that can lead to stronger and more biocompatible stents. There is a need for stents that have high radial strength which will greatly increase the clinical success rate and decrease the chance of restenosis and other complications. According to literature, there is a great need for advanced stent designs. Potential stent developments can help improve the quality of life in patients affected by atherosclerosis. For example, current research studies involve using biodegradable PLLA (poly-L-Lactide) stents that are absorbed into the body after a given time period [14], [20]. These stents could also be drug eluting. Drug eluting stents release medicine that can help prevent a redisposition of plaque. Both biodegradable stents and drug eluting stents could possibly decrease the risk associated with restenosis.

There are two main types of stents. These types include balloon expandable (Figure 1) and self-expandable (Figure 2). A balloon expandable stent is crimped onto a balloon and guide wire. The stent travels on the balloon/guide wire combination to the affected area. A pressure is then applied to the balloon, which then expands. The balloon expansion in turn expands the stent to a specified diameter (depending upon the applied pressure).

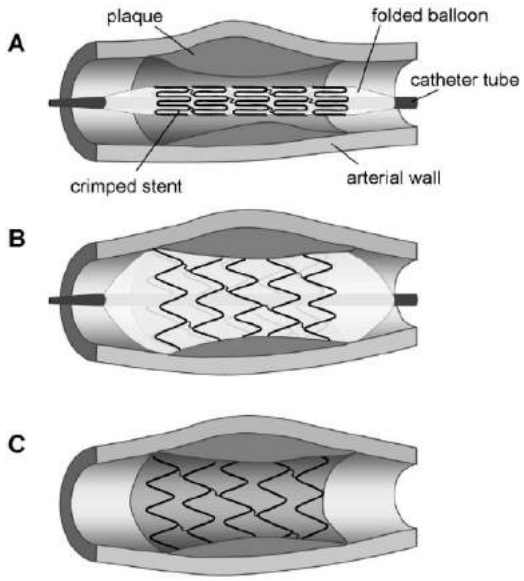

Fig. 1: Schematic illustration of a balloon-expandable stent placement [16].

As seen in Figure 1, after a stent has been properly positioned (A), the balloon is inflated at high pressure leading to the expansion of the device and to an improved luminal area (B). The balloon catheter is deflated and extracted and the stent remains in place to keep the vessel open (C) [16].

The second type of stent is a self-expandable stent. Self-expanded stents are manufactured to their major diameter and then crimped. The crimped stent is then constrained to the guide wire [23]. The constraint is removed once the stent reaches the target artery. The stent then returns to its pre-manufactured diameter by recovering its strain. Figure 2 shows a schematic of the deployment of a self-expandable stent.

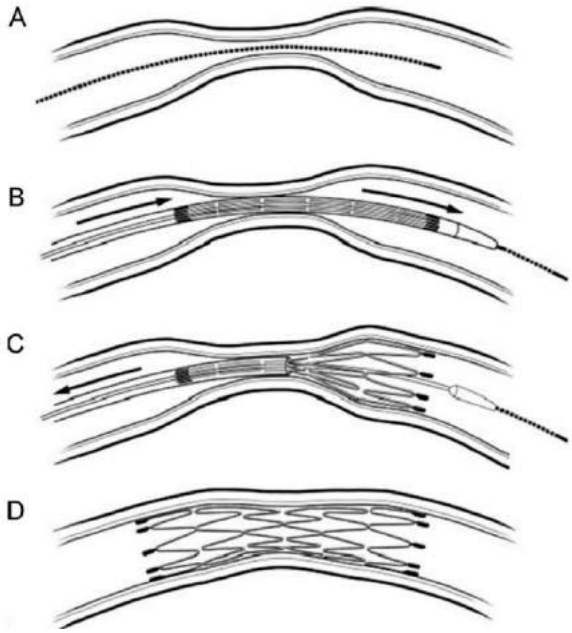

Fig. 2: Illustration of the steps involved in self-expanding stent delivery and deployment [10].

In the first step, a steerable wire is softly advanced across the stenotic lesion (A). The undeployed stent is delivered to the target (B) after a small balloon angioplasty. The stent is deployed distally in a proximal fashion by removing the sheath (C). A completely deployed stent is hence placed in the diseased portion of the artery (D) [10].

However, stents can have their own associated health concerns. The major concern with stents is the chance of restenosis [22]. Stenting adds stress to the arterial wall that can lead to arterial wall shearing after stent deployment within the artery. These stresses and shearing, in turn, can lead to arterial wall remodeling. Arterial wall remodeling occurs when endothelial cells attempt to recover the injuries caused by stenting [14]. This reaction is an inflammatory endothelial reaction to the shearing caused by the stent expansion and can lead to luminal loss. Stenosis then can reoccur and block the arterial passageway.

Stent design is a critical factor in clinical success. It has been noted in literature that poor stent design can lead to rather undesirable clinical outcomes [19]. Radial strength determines the pressure that the stent can withstand [7]. A stent with insufficient radial strength can lead to arterial damage; can collapse if the critical pressure for the design is exceeded [7]; and can also cause injury if it does not expand properly. A stent that expands past it major diameter will shear the arterial wall. The

endothelial process can then try to recover the damage caused to the artery. A stent that does not expand to its major diameter will result in lower luminal gain. This will decrease the downstream blood flow to the heart.

Stent material is also an important factor in determining a stent's clinical success. Research has shown that stents that utilize a material with a low coefficient of friction will limit bacterial formation around the stented site [2]. Material is the major factor in determining the stent's biocompatibility which is the inability of a material to induce an immunological response in-vivo [11]. A stent that makes use of an incompatible material will lead to immunity response that can lead to inflammation around the stented area [11]. Vascular scarring can also occur. This can further lead to toxin buildup around the stent that can kill healthy cells. The material can also corrode, leading to a more substantial buildup of toxins.

Design Simulation and Experimental Design techniques are being widely used these days in the product design process for biomedical devices such as stents in order to develop robust designs [4-5], [8-9]. A robust design meets all functional requirements of the product with little variability in its in-vivo performance. In this paper, we propose a methodology that is based on combination of design simulation and experimental design to study the effect of strut design and material on the robustness of the coronary stents.

2 PROBLEM STATEMENT

Various coronary stent designs exist in the market. Additionally, several different materials are being used in stent manufacturing. The stents are exposed to several pressures once they are placed inside the human body. These pressures include the deployment pressure to expand the stent to conform to the arterial wall, the pressure associated with the heartbeat, the pressure exerted by the arterial wall, and the pressure exerted by the offending plaque. In this paper, we focus only on the pressures that are exerted on the stent by the arterial wall. A stent that fails when exposed to pressure can cause significant health risks including restenosis and arterial wall shearing.

Restenosis can be a serious condition. If restenosis happens, a heart attack or stroke (depending on the stent location) can occur because of arterial blockage. Re-stenting is a possibility to remedy restenosis. Re-stenting occurs when a stent is placed within another stent. However, if stents are designed properly, restenosis rates can be significantly reduced. Previous research has shown that thinner strut thickness add less stress to the arterial wall [24]. This decreases damage to the arterial wall and decreases the chance for restenosis occurrence. However, there are tradeoffs involved with the thinner strut designs. A stent designed with thin struts will recoil after it is expanded. Recoil occurs when the structural integrity of the design cannot overcome the inherent strain energy associated with the material. This results in lower gain in the arterial lumen and decreased blood flow gain [24].

This paper compares different combinations of strut designs and material types. It is hypothesized that both strut design and material play a significant role in determining the radial strength of the stent. The strut design determines the stent's structural integrity. The material's yield strength determines the stress at which the material undergoes plastic deformation. Once a material undergoes plastic deformation it cannot recover to its original size. Thus, both strut design and material impact stent strength. The goal is to determine the appropriate combination of stent strut design and material which will lead to a stent that can properly be exposed to in-vivo pressures.

3 METHODOLOGY

A 3^2 full factorial design was used to study and analyze the effect of strut design and material on the stent strength. The Von Mises stress was used as the response variable to measure the stent strength. The input factors considered were stent cell design and the stent material. Each factor has three levels. The stent cell design includes an open stent design, a sinusoidal cell design, and a Palmaz design. Three different materials were considered: Nitinol, 316 stainless steel, and poly-l-lactic acid. These three materials are most commonly used in today's commercially available stents.

Figure 3 illustrates the three important phases in the design methodology that was used. The first phase involved creating three dimensional CAD models of the stent designs using a parametric CAD software package. The stents were modeled in a fully expanded state. A stent's fully expanded state occurs when the stent is deployed within the lumen. The fully expanded state represents the stent's largest diameter.

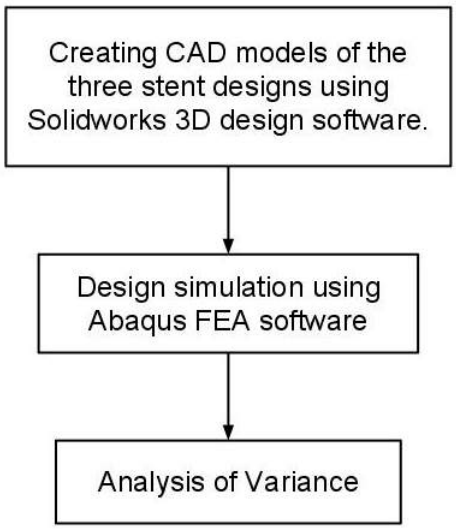

Fig. 3: Three key phases in the design methodology.

The second phase involved performing a design simulation using Abaqus® finite element analysis (FEA) software. Static FEA analysis was performed in which time variations were ignored. Rather, an instantaneous uniformly distributed pressure was applied to the stent. The first step in an FEA simulation is to apply boundary conditions. Boundary conditions are the constraints that are applied to the model in order to simulate real-life limitations of motion with respect to the various degrees of freedom. In this simulation, the stent was axially fixed. This boundary condition was used in order to simulate friction holding the stent in place [2]. Loads must also be applied to the model. The human artery has a pressure of 175 mm Hg (0.02333 MPa) [15]. This pressure was applied to the exterior surface of the stent model to simulate the artery pressure.

The stent model was meshed using a tetrahedral element profile. A tetrahedral element consists of 10 nodes. A large number of nodes help to increase the accuracy of the stress analysis. Different seeds were used to randomize the meshing profile for the simulation. Two seeding factors (1.0 for replicate one and 1.1 for replicate two) were used in order to create replicates for the experimental

design. Seeding controls the relative size of individual element of the mesh. As the seed number decreases, the element size also decreases. The decreased size of the mesh element leads to a larger number of elements in the mesh. Thus, the seeding process determines the mesh density.

Once the FEA simulation was completed, the obtained data was analyzed using the Abaqus CAE postprocessor. The Abaqus postprocessor provides a visual representation of the stresses present within the design. The postprocessor also provides a text based report that presents the maximum Von Mises stress present in the model.

The third phase involved performing analysis of variance (ANOVA) on the maximum Von Mises stress values obtained for various combinations of strut design and material. Two-way ANOVA was used to examine the influence of strut design, type of material, and the interaction effect between these two factors on the Von Mises stresses generated around the stent.

4 COMPUTER AIDED DESIGN

Commercially available stents come in a variety of shapes and sizes depending on the application. The stents that we modeled in this paper use a similar size factor. The three stent CAD models were created using similar lengths, expanded diameters, and strut thickness. It is necessary to use the same dimensions to generate meaningful results. The results would be skewed if the stents were modeled using non-uniform dimensions. For example, a stent with thicker struts would have lower residual stresses than a corresponding stent with thin struts.

The stents were modeled in a fully expanded state. A strut thickness of 0.009 inches was utilized for each stent design. The diameters and length for each stent were modeled to be the same dimension. Figure 4 provides isometric views of the three stent designs: Palmaz® design, Sinusoidal design, and open stent design respectively.

(a) (b) (c)

Fig. 4: CAD model of (a) Open stent design, (b) Sinusoidal stent design, and (c) Palmaz® stent design.

Stents are typically manufactured using computer numerical codes with automated lasers. Due to its unique capabilities, laser processing has become the predominant method of cutting, ablating, and welding materials for stent manufacturing. Compared to other cutting methods, laser processing produces very smooth edges that substantially reduce the finishing process. Another advantage for laser processing is its unique ability to make intricate design cuts with extreme precision and accuracy [1]. The lasers use a converted two dimensional geometry to create the three dimensional stent. The stents were modeled in a similar manner. The flat pattern was first drawn to include the struts and connecting bridge and was then wrapped around a cylinder. Figure 5 shows an example of the flat pattern and its corresponding cylinder for the sinusoidal stent.

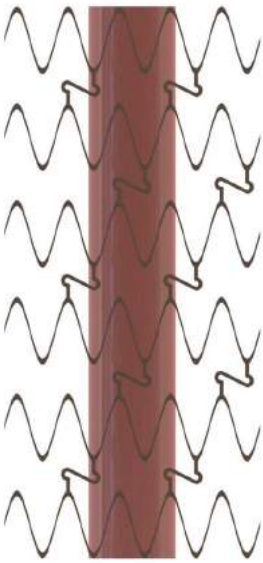

Fig. 5: Flat Pattern and Cylinder for Sinusoidal Stent.

The width of the flat pattern corresponded to the circumference of the wrapped stent. The following equation shows this relationship.

$$L = C = \pi D$$

Where, L is the overall pattern length
C is the overall stent circumference
D is the stent diameter

The flat pattern was then wrapped around a circle with a diameter equal to the flat pattern length divided by **Ù**.

For sinusoidal stent design, following equation was used to determine the size and shape of the cell pattern. The equation was used to find the x and y coordinates for the sine curve.

$$y(x) = 0.07 \sin\left(\left(\frac{2\pi}{0.14}\right)(x - 0.07)\right) + 0.07$$

5 DESIGN SIMULATION

In our FEA analysis, we did not take into account the periodic nature of the heartbeat. A heart beat can be thought of a sinusoidal wave. The pressure was applied to the stent in correspondence with the peak amplitude of the sinusoidal wave function. Additionally, the full super-elastic nature of nitinol stenting materials was not modeled. Materials used in nitinol stents are usually able to recover a percentage of their strain after they transition to a plastic deformation phase due to an austenitic and martensitic transformation. The materials were modeled using elastic properties such as Youngís Modulus and Poissonís Ratio. The super-elastic nature of the nitinol materials and periodic nature of the heart beat is the topic for future research.

Material properties for the three testing materials were input into the Abaqus material database. Nitinol has a Youngís Modulus of 24 GPA and yield strength of 124 MPA [6]. There are various grades of 316 stainless steel. The grade that was used for this experiment is Carpenter BioDur 316LS Stainless Medical Implant Alloy (Annealed) [12]. This stainless steel alloy has an ultimate tensile strength of 586 MPa and a yield strength of 434 MPa. PLLA is another material of interest. It has an ultimate tensile strength of 900 MPa and a Youngís modulus of 8.5 GPa [13].

As explained earlier, most materials used in stent design tend to be materials that have a larger elastic region (higher modulus of resilience). However, because of the nature of this static study, the materials could be modeled to represent an instantaneous state. The materials were defined by entering the corresponding Youngís Modulus and Poissonís Ratio. The stents were assigned homogenous, solid material properties. Appropriate boundary conditions were applied next. The stents were fixed at the ends to simulate friction holding the stents against the arterial wall. An encastre boundary condition was applied to allow for zero degrees of freedom along the X, Y, and Z axes. A uniformly distributed pressure of 0.02333 MPa was applied to the periphery of the stent. The compressive stress was induced on the stent using the negative vector value in Abaqus. This simulates the pressure applied by the arterial wall. Figure 6 shows the boundary and loading conditions for each stent model. The red color indicates the location of the uniformly distributed pressure. The orange color indicates the locations of the encastre boundary condition. The encastre boundary condition confines the translational and rotational degrees of freedom for the X, Y, and Z axes to zero. A zero degree of freedom restrains rotations and translations.

The selection of three different stent designs along with three different materials created nine different scenarios in total for the FEA analysis. A mesh was applied to each scenario. A tetrahedral element was used for the mesh control. Two different global seeds were used in order to create two replicates for each scenario. A global seed of 1.0 was used for the first replicate. A global seed of 1.1 was used for the second replicate. Replicates provide more data points for the analysis. Figure 7 shows examples of tetrahedral meshing for the open stent model, sinusoidal stent model, and Palmaz stent model respectively.

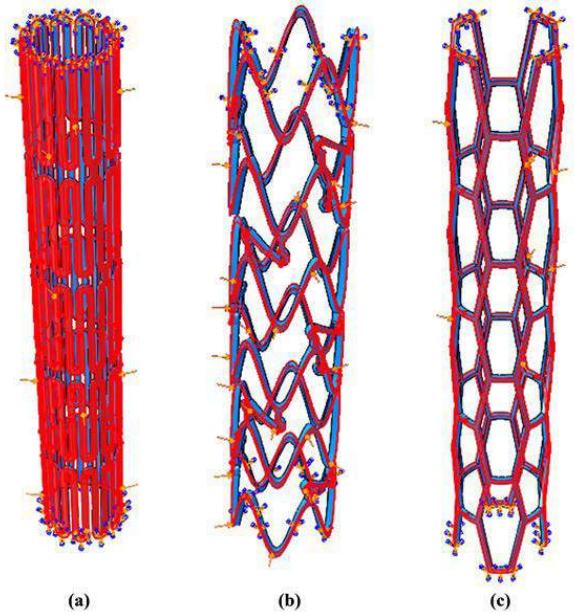

Fig. 6: Boundary and loading conditions for (a) Open stent, (b) Sinusoidal stent, and (c) Palmaz stent.

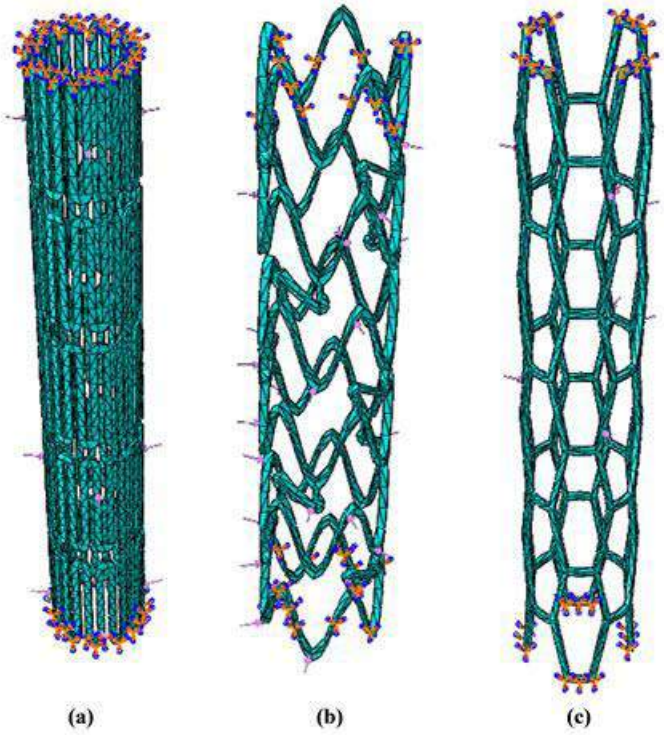

Fig. 7: Examples of meshing for (a) Open stent, (b) Sinusoidal stent, and (c) Palmaz stent.

After completion of the meshing process, the Abaqus postprocessor was used to plot the Von Mises stresses. The Abaqus report was used to record the maximum Von Mises stress for each design scenario. Figures 8 through 10 show the visual plots of the Von Mises stress for each combination of strut design and material. These figures provide a graphical method of explaining the Von Mises stresses in the stent. Areas that are shown in blue have low Von Mises stress concentrations. The Von Mises stresses increase as you move along the color bar. Red color would indicate the highest Von Mises stress present. The detailed statistical analysis is performed in the next section.

Figure 8 demonstrates the Von Mises stresses for the open stent design. It can be observed from Figure 8 that the maximum Von Mises stresses occur at the radii on the stent struts. This concentration is likely due to radii acting as stress concentration points. The struts are designed in such a way as to reduce the stresses on the load-bearing portions of the struts.

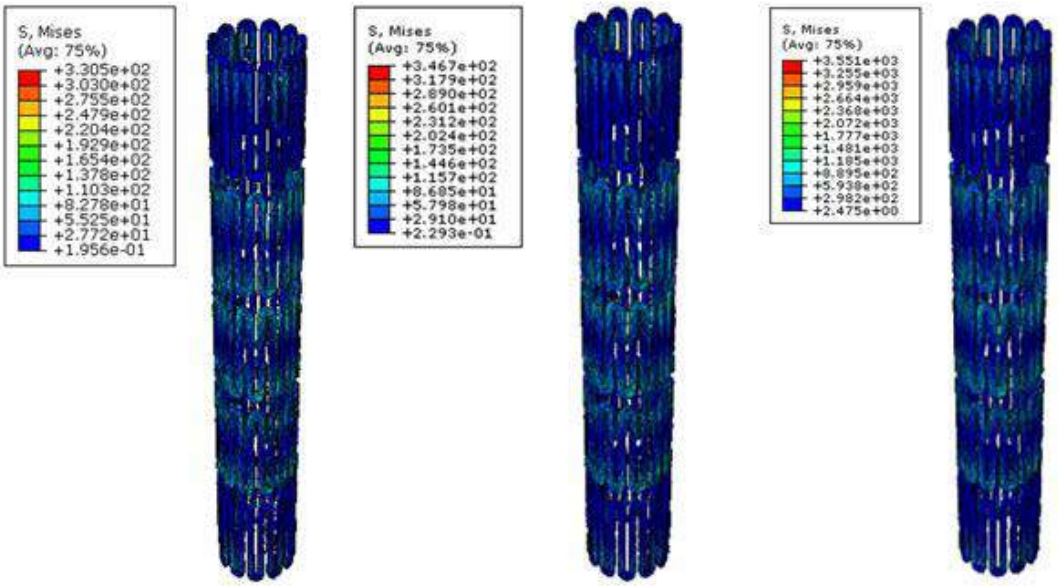

Fig. 8: Von Mises Stress (MPa) for open Stent with 316 Stainless Steel, Nitinol, and PLLA respectively.

Figure 9 demonstrates the Von Mises stresses for the sinusoidal stent design. It is clear from Figure 9 that the stresses are localized at the connection points between the stent struts and bridges. The transition that occurs between the bridges and the struts is very sharp. There is no radius to ease the transition. The sharpness leads to stress concentration and possible crack propagation.

Figure 10 demonstrates the Von Mises stresses for the Palmaz stent design. Figure 10 shows that the maximum Von Mises stresses occur at the connections between struts. This stent is a closed cell design. Each strut is connected to the adjacent strut. The connections provide stress concentration. Another observation from Figure 10 is that the Palmaz stent design appears more robust as compared to the open and the sinusoidal stent designs. This is likely because of its closed cell structure.

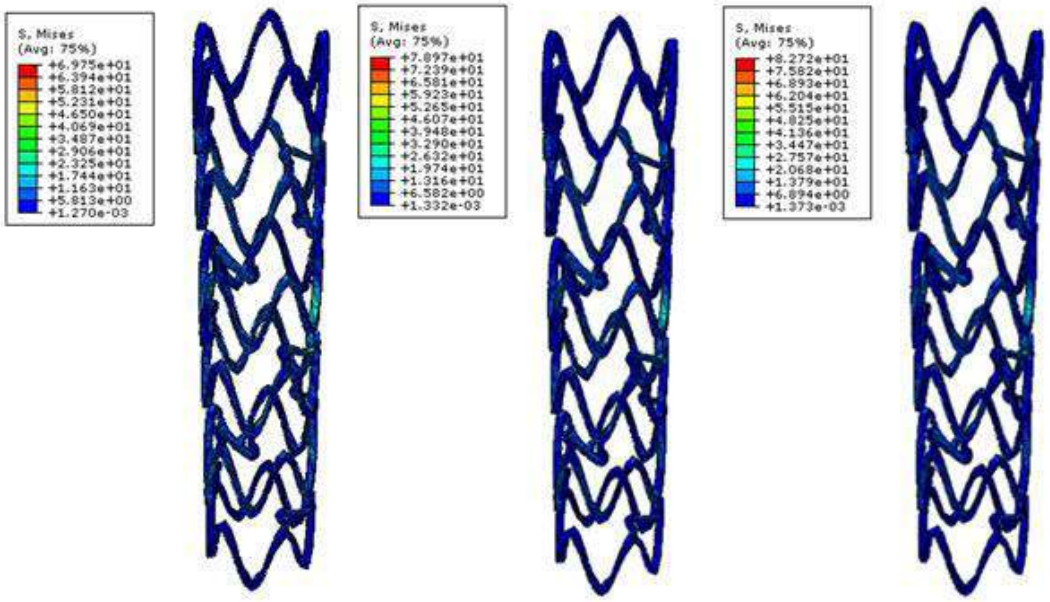

Fig. 9: Von Mises Stress (MPa) for Sinusoidal Stent with 316 Stainless Steel, Nitinol, PLLA respectively.

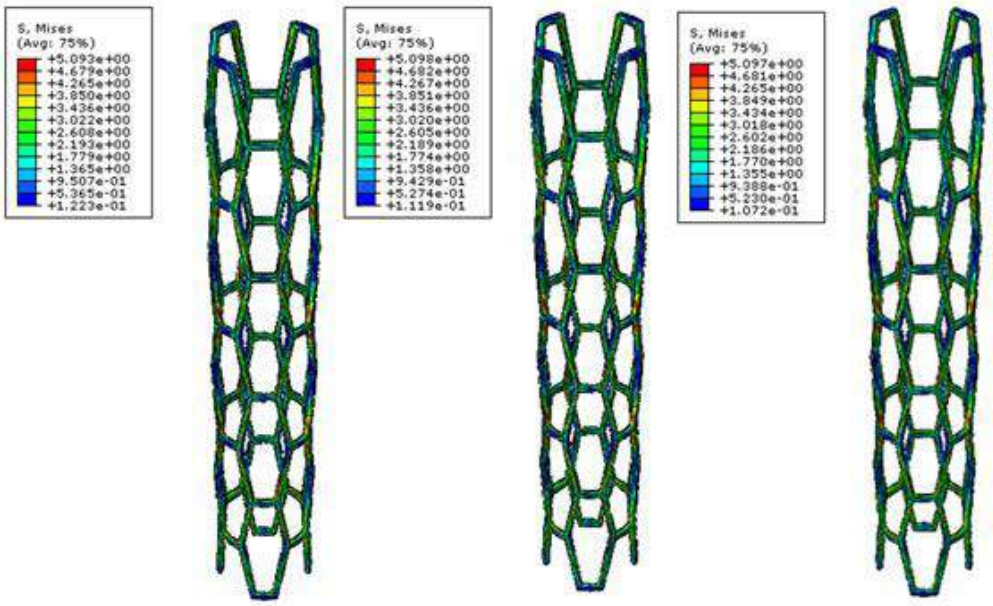

Fig. 10: Von Mises Stress (MPa) for Palmaz Stent with 316 Stainless Steel, Nitinol, PLLA respectively.

6 STATISTICAL ANALYSIS AND FINDINGS

Table 1 shows maximum Von Mises stress values obtained from the Abaqus postprocessor for each combination of the strut design and material. Two replicates were used for each scenario.

Strut Design	Material		
	316 Stainless	*Nitinol*	*PLLA*
Open	146.913	145.376	145.825
	144.374	149.615	151.704
Sinusoidal	36.6813	39.4477	40.9226
	28.3869	28.1597	27.9133
Palmaz	4.56362	4.55113	6.04242
	4.55324	4.54363	4.53841

Tab. 1: Maximum Von Mises Stresses in MPa.

These results were then analyzed using the two-way ANOVA [15]. The analysis was performed to determine the main effects and interaction effects. A confidence level of 95% was used. The response variable was maximum Von Mises Stress generated around the stent. The two input factors were strut design and material type. Each of these factors has three levels as shown in Table 1. Table 2 shows the mean values of Von Mises stresses for the various factor level combinations and Table 3 shows the standard deviation values for the various factor level combinations

ANOVA Sample Means	316 Stainless	Nitinol	PLLA	Totals
Open	145.64	147.50	148.76	147.30
Palmaz	4.56	4.55	5.29	4.80
Sinusoidal	32.53	33.80	34.42	33.59
Totals	60.91	61.95	62.82	

Tab. 2: Mean values of Von Mises Stresses in MPa. for the various factor level combinations.

ANOVA Sample Std Dev	316 Stainless	Nitinol	PLLA	Totals
Open	1.80	3.00	4.16	2.81
Palmaz	0.01	0.01	1.06	0.61
Sinusoidal	5.87	7.98	9.20	6.11
Totals	66.87	67.65	67.98	

Tab. 3: Standard deviation values for the various factor level combinations.

Table 4 shows the ANOVA output. The P value from the ANOVA output is used to determine if a factor is significant. There are three important P values in Table 4: two for main effects of the strut design and the material type and one for the interaction between these two factors. Strut design has a P value close to zero. This is less than the confidence value of 0.05. Therefore, we can conclude that the strut

design has significant impact on the Von-mises stresses generated around the stent. The material factor has a P value of 0.798. This is greater than the confidence level; therefore we can conclude that the material type has no impact on the stresses generated around the stent. The interaction between factors should also be examined. The interaction has a P value of 0.997. This is again greater than the confidence level. Thus, the interaction effect between strut design and material is insignificant as well.

Source	Sum of Squares	Degrees of Freedom	Mean Squares	F-Ratio	P-value
Strut Design	68133.83	2	34066.91	1437.09	< 0.0001
Material	11.00	2	5.50	0.23	0.7976
Interaction	3.27	4	0.82	0.03	0.9973
Error	213.35	9	23.71		
Total	68361.45	17			

Tab. 4: ANOVA output.

The residuals from a factorial experiment play an important role in assessing model adequacy. Figure 11 shows the normal probability plot of the residuals. There is no indication of non-normality. Also, there is no indication of possible outliers. Figure 12 shows the residuals versus the fitted values. This plot shows no special trends indicating that there is no relationship between the size of the residuals and the fitted values.

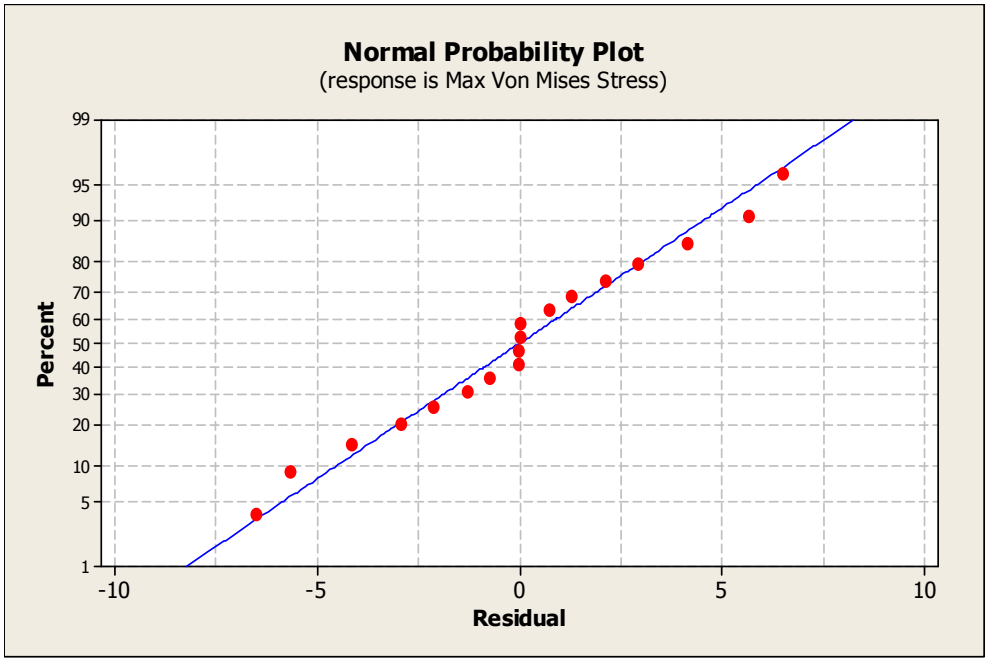

Fig. 11: Normal probability plot of residuals.

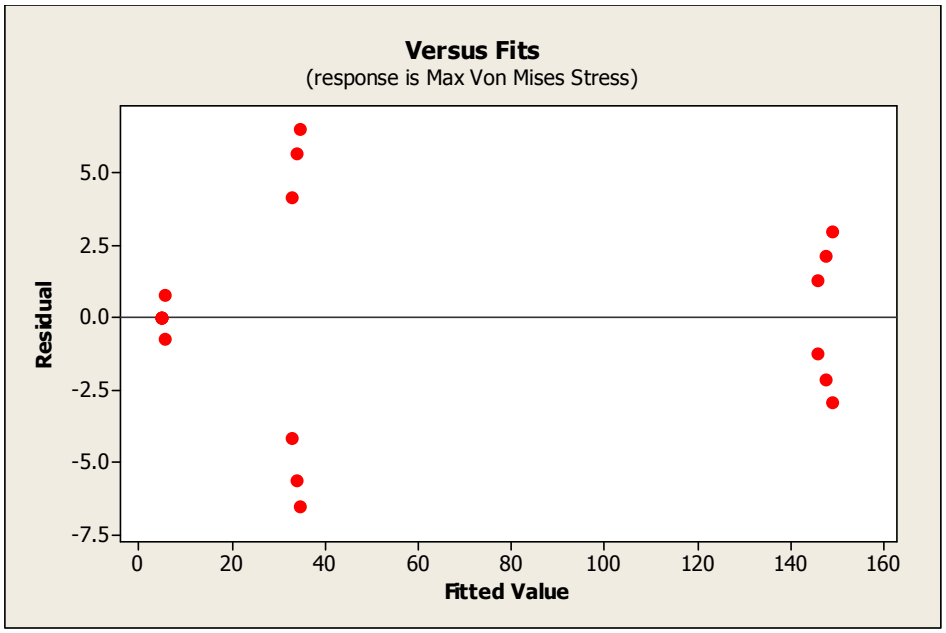

Fig. 12: Plot of residuals versus fitted values.

Figures 13 and 14 show the interaction plots. The lines in different colors are parallel to each other in both the plots indicating that the interaction effect between the strut design and the material is not significant. Additionally, we can also conclude from Figure 13 that the Palmaz design is the most effective and the open strut design is the least effective in minimizing the Von Mises stress (shown on the Y-axis). It is also clear from Figure 14 that the material type is insignificant since the Von Mises stress values for different material types are almost the same.

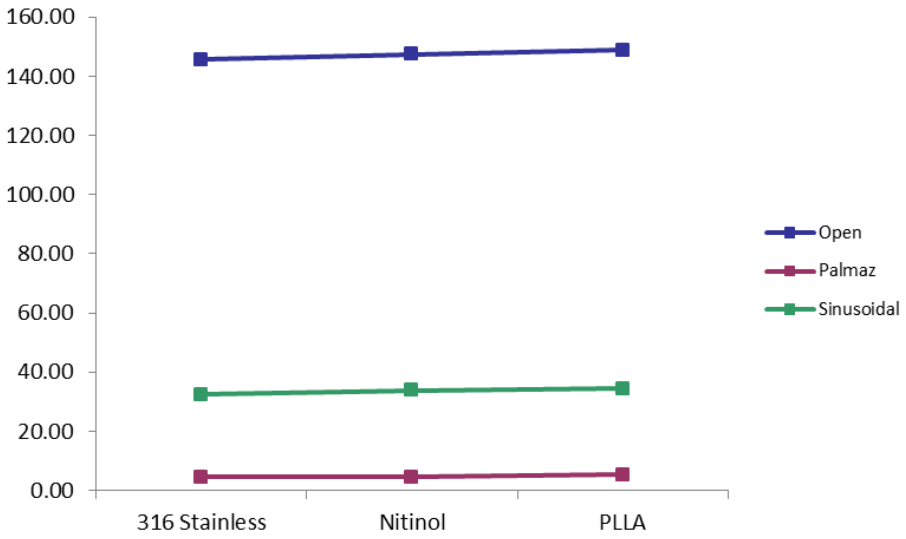

Fig. 13: Interaction plot: Strut Design by Material.

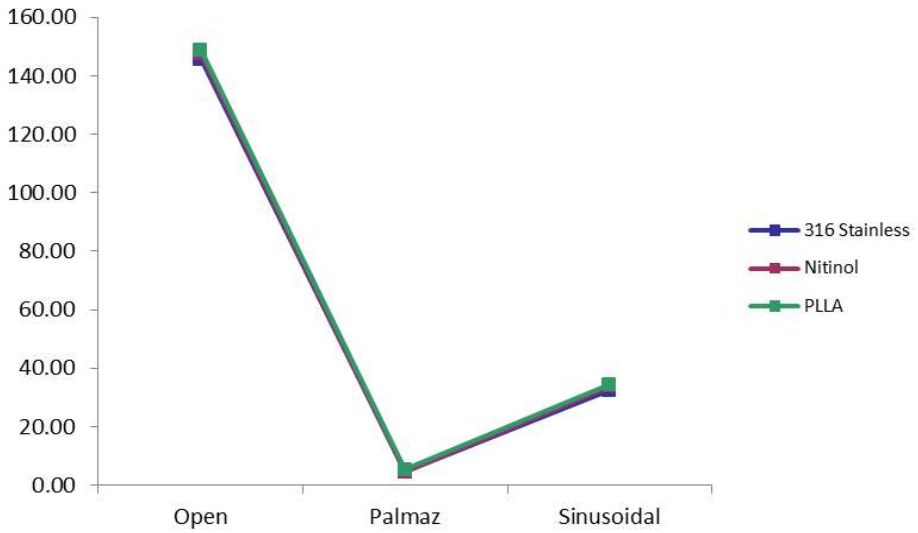

Fig. 14: Interaction plot: Material by Strut Design.

Thus, the findings of this research indicate that strut design is the sole factor in determining the maximum Von Mises stress induced by arterial wall pressure. Material is not a significant factor. However, according to previously cited literature, material is an important factor in determining biocompatibility of the stent. Material is also an important factor is determining a stent's fatigue life.

7 CONCLUSION AND FUTURE RESEARCH

The findings refute the hypothesis that strut design and material are both significant factors in determining stresses induced by arterial wall pressure. The findings indicate that the Palmaz stent is most capable of withstanding arterial wall pressure. It is well documented in literature that the Palmaz stent has a high level of safety [21] and has been clinically proven to reduce in-vivo complications such as restenosis. The findings in this research support the fact that the Palmaz stent is a clinically safe stent strut design. The diamond shaped cells of a Palmaz stent provide a high degree of structural integrity. The open stent design would be the least capable of withstanding arterial wall pressure

Experimental design studies are sequential in nature. This study was mainly focused on two parameters: strut design and material type. With the findings of the current study, it is possible now to perform subsequent experiments on Palmaz stent design focusing on its other sophisticated design parameters, different loading and pressure conditions, actual arterial shape, etc. Future research will expand the analysis to a dynamic study. The dynamic study will involve all forces and pressures that are associated with stents. These pressures and forces include deployment forces, periodic blood pressure, and pressures from the arterial wall. The future research will also analyze the impact on the arterial wall. This part of the research will determine the shear and displacement on the arterial wall. The potential for restenosis can then be determined.

Currently we are undertaking another study to determine the fatigue life of varying stent geometries. The stents will be expanded in an artery model. A sinusoidal service loading equivalent to the pulse pressure will be applied to the inner surface of the artery and stent. The maximum and

minimum principle stresses will be monitored to determine the number of reversible loads (using stress life theory and strain life theory).

In the current study, the strut thickness was a held-constant factor because we were mainly interested in studying the effect of stent design and material type on its robustness. With the findings in the current paper, a subsequent parametric study using SolidWorks design studies can also be performed on the Palmaz design to analyze the impact of varying strut thickness on stresses generated around the stent. Strut thickness has significant impact on stent stresses. A thicker strut will generally have lower stresses due to an increase in the stentôs second moment of inertia. The thickness study can be combined with a study in which the stents are expanded within the artery. It is well known that thicker stent struts can lead to higher shear stresses within the artery wall. High arterial stress levels can lead to restenosis (or a re-closure of the artery).

REFERENCES

[1] Aerotech Inc., Pittsburgh, PA (edited by Modic, Elizabeth Engler) : Laser processing in stent production, Todayôs Medical Developments (TMD), 5(2009), 36-40, http://www.onlinetmd.com/Magazine/Default.aspx

[2] Alicea, L.; Aviles, J.; Lopez, I.; Mulero, L.; Sanchez, L.: Mechanics Biomaterials: Stents, Applications of Engineering Mechanics in Medicine, GED ð University of Puerto Rico, Mayaguez, 2004.

[3] American Heart Association: Cardiovascular Disease Statistics, Retrieved February 24, 2011, http://www.americanheart.org/presenter.jhtml?identifier=4478.

[4] Buchter, A.; Wiechmann, D.; Koerdt, S.; Wiesmann, H.P.; Piffko, J.; Meyer, U.: Load-related implant reaction of mini-implants used for orthodontic anchorage, Clinical Oral Implants Research, 16 (4), 2005, 473-479, http://dx.doi.org/10.1111/j.1600-0501.2005.01149.x

[5] Chang, P.B.; Williams, B.J.; Bhalla, K.S.; Belknap, T.W.; Santner, T.J.; Notz, W.I.; Bartel, D.L.: Design and analysis of robust total joint replacements: finite element model experiments with environmental variables, Journal of Biomechanical Engineering, 123(3), 2001, 239-46, http://dx.doi.org/10.1115/1.1372701.

[6] Domingo, S.; Puertolas, S.; Gracia-Villa, L.; Mainar, M.; Uson, J.; Puertolas, J.: Design, manufacture and evaluation of a NiTi stent for colon obstruction, Bio-Medical Materials and Engineering, 15 (5), 2005, 357-365.

[7] Duerig, T.W.; Wholey, M.: A comparison of balloon- and self-expanding stents, Minimally Invasive Therapy and Allied Technologies, 11(4), 2002, 173-178, http://dx.doi.org/10.1080/136457002760273386.

[8] Early, M.; Lally, C.; Prendergast, P.J.; Kelly, D. J.: Stresses in peripheral arteries following stent placement: a finite element analysis, Computer methods in Biomechanics and Biomedical Engineering, 12(1), 2009, 25-33, http://dx.doi.org/10.1080/10255840802136135.

[9] El-Haik, B.; Mekki, K.S.: Medical Device Design for Six Sigma: A Road Map for Safety and Effectiveness (2 ed.). Wiley-Interscience, 2008.

[10] Guo, Xin-bin; Ma, Nan; Hu, Xiao-bo; Guan, Sheng; Fan, Yi-mu: Wingspan stent for symptomatic M1 stenosis of middle cerebral artery, European Journal of Radiology, 80, 2011, e356-e360.

[11] Lim, I.: Biocompatibility of Stent Materials. MIT Undergraduate Research Journal, 11, 2004, 33-37.

[12] MatWeb: Carpenter BioDurÊ 316LS Stainless Medical Implant Alloy, Annealed, Retrieved from Material Property Data, 1999, http://www.matweb.com/search/DataSheet.aspx?MatGUID=7c75fbd84f4245318c6da363da395d70

[13] MatWeb: *Poly-L-lactide (PLLA)*, Retrieved from Material Property Data, 1999, http://www.matweb.com/search/DataSheet.aspx?MatGUID=29b34b1e179648339cc08166f2165ab9.

[14] Meng, B.; Wang, J.; Zhu, N.; Meng, Q.Y.; Cui, F.Z.; Xu, Y.X.: Study of biodegradable and self-expandable PLLA helical biliary stent in vivo and in vitro, Journal of Materials Science: Materials in Medicine, 17(7), 2006, 611-617, http://dx.doi.org/10.1007/s10856-006-9223-9.

[15] Montgomery, D.: Design and Analysis of Experiments (7 ed.). John Wiley and Sons, Inc., 2009.

[16] Mortier, Peter: Computer Modeling of Coronary Bifurcation Stenting, Ph.D Dissertation, Institute Biomedical Technology, Univesiteit Gent, Ghent, Belgium, 2010.

[17] Palmaz, J. C.: Influence of stent design on clinical outcome, Minimally Invasive Therapy and Allied Technology, 11 (4), 2002, 179-183, http://dx.doi.org/10.1080/136457002760273395.

[18] Perry, M.; Oktay, S.; Muskivitch, J.: Finite element analysis and fatigue of stents, Minimally Invasive Therapy and Allied Technologies, 11(4), 2002, 165-171, http://dx.doi.org/10.1080/136457002760273377.

[19] Prabhu, S.; Feezor, C.; Denison, A.; Rebelo, N.; Serrar, M.: Deployment of a self-expanding stent in an artery, ABAQUS Users' Conference, 2004.

[20] Saito, Y.; Tanaka, T.; Andoh, A.; Minematsu, H.; Hata K.; Tsujikawa, T.; Nitta, N.; Murata, K.; Fukiyama, Y.: Novel biodegradable stents for benign esophageal strictures following endoscopic submucosal dissection, Digestive Diseases and Sciences, 53(2), 2008, 330-333, http://dx.doi.org/10.1007/s10620-007-9873-6.

[21] Serruys, P.: Handbook of Coronary Stents, Martin Dunitz, London, 1997.

[22] Timmins, L.; Mereno, M.; Meyer, C.; Criscione, J.; Rachev, A.; Moore, J.: Stented artery biomechanics and device design optimization, Medical and Biological Engineering and Computing, 45(5), 2007, 505-513. http://dx.doi.org/10.1007/s11517-007-0180-3.

[23] Wholey, M.H.; Wholey, M.H.; Tan, W.A.; Eles, G.; Jarmolowski, C.; Cho, S.: A comparision of ballon-mounted and self-expanding stents in the carotid arteries: immediate and long-term results of more than 500 patients, Journal of Endovascular Therapy, 10(2), 2003, 171-181, http://dx.doi.org/10.1583/1545-1550(2003)010<0171:ACOBAS>2.0.CO;2.

[24] Zahedmanesh, H.; Lally, C.: Determination of the influence of stent strut thickness using the finite element method: implications for vascular injury and in-stent restenosis, Medical and Biological Engineering and Computing, 47(4), 2009, 385-393, http://dx.doi.org/10.1007/s11517-009-0432-5.